0090-9556/11/3901-151–159$20.00
DRUG METABOLISM AND DISPOSITION
Vol. 39, No. 1
35105/3655512
DMD 39:151–159, 2011
Printed in U.S.A.

Identification of Clinically Used Drugs That Activate Pregnane X Receptors[S]

Sunita J. Shukla, Srilatha Sakamuru, Ruili Huang, Timothy A. Moeller, Paul Shinn, Danielle VanLeer, Douglas S. Auld, Christopher P. Austin, and Menghang Xia

National Institutes of Health Chemical Genomics Center, National Human Genome Research Institute, National Institutes of Health, Bethesda, Maryland (S.J.S., S.S., R.H., P.S., D.V.L., D.S.A., C.P.A., M.X.); and Celsis in Vitro Technologies, Halethorpe, Maryland (T.A.M.)

Received June 22, 2010; accepted October 21, 2010

ABSTRACT:

The pregnane X receptor (PXR) binds xenobiotics and regulates the expression of several drug-metabolizing enzymes and transporters. Human PXR (hPXR) activation and CYP3A4 induction can be involved in drug-drug interactions, resulting in reduced efficacy or increased toxicity. However, there are known species-specific differences with regard to PXR activation that should be taken into account when animal PXR data are extrapolated to humans. We profiled 2816 clinically used drugs from the National Institutes of Health Chemical Genomics Center Pharmaceutical Collection for their ability to activate hPXR and rat PXR (rPXR) at the cellular level, induce human CYP3A4 at the cellular level, and bind human PXR at the protein level. From 6 to 11% of drugs were identified as active across the four assays, which included assay-specific and pan-active compounds. The lowest concordance was observed between the hPXR and rPXR assays, and many compounds active in both assays nonetheless demonstrated significant potency differences between species. Analysis based on clustering potency values demonstrated the greatest activity correlation between the hPXR activation and CYP3A4 induction assays. Structure-activity relationship analysis identified chemical scaffolds that were pan-active (e.g., dihydropyridine calcium channel blockers) and others that were uniquely active in individual assays (e.g., steroids and fatty acids). These results provide important information on PXR activation by clinically used drugs, highlight the species specificity of PXR activation by xenobiotics, and provide a means of prioritizing compounds for follow-up studies and optimization efforts.

Introduction

The pregnane X receptor (PXR) is a member of the nuclear receptor (NR) family, based on its sequence homology to other NRs (Kliewer et al., 1998). PXR is expressed in the intestine and liver across species (Kliewer, 2003) and plays a critical role in the regulation of genes involved in drug metabolism and efflux (LeCluyse, 2001; Ekins and Schuetz, 2002; Ekins et al., 2008), most notably cytochrome P450 (P450) enzymes, glutathione transferases (GSTs) and multidrug resistance protein 1 (Kliewer, 2003). Unlike other nuclear receptors, the PXR ligand-binding domain (LBD) is largely hydrophobic and extremely flexible, thus allowing for conformational changes to accommodate structurally diverse molecules (Watkins et al., 2001). Structurally diverse PXR ligands include antibiotics, calcium channel blockers, steroids, dietary supplements, environmental pollutants, antimycotics, protease inhibitors, and statins (Blumberg and Evans, 1998; Kliewer et al., 1998; Jones et al., 2000; Goodwin et al., 2002; Zhang et al., 2008).

Several studies have identified PXR as an important regulator of CYP3A4, involved in the metabolism of more than 50% of all prescribed drugs in humans with the aid of various coactivators (Fig. 1A) (Lehmann et al., 1998; Jones et al., 2000; Sinz et al., 2008). The ability of PXR to bind a broad range of substrates has been shown to correlate with the induction of CYP3A4 expression (Timsit and Negishi, 2007). PXR activation and CYP3A4 induction are involved in approximately 60% of all drug-drug interactions (Evans, 2005), in which an administered drug modulates the metabolism of a coadministered drug, leading to decreased efficacy or increased toxicity.

Most DNA-binding domains of mammalian PXR receptors are highly conserved (95% identity); however, the PXR LBD is highly divergent across species, sharing roughly 70% sequence identity (Jones et al., 2000; Moore et al., 2000). This divergence, noted by specific amino acid differences in the crystal structure of the PXR LBD (Ekins and Schuetz, 2002), plays a role in species-specific

This research was supported in part by the Intramural Research Program of the National Institutes of Health National Human Genome Research Institute.

Article, publication date, and citation information can be found at http://dmd.aspetjournals.org.

doi:10.1124/dmd.110.035105.

[S] The online version of this article (available at http://dmd.aspetjournals.org) contains supplemental material.

ABBREVIATIONS: PXR, pregnane X receptor; NR, nuclear receptor; P450, cytochrome P450; GST, glutathione transferase; LBD, ligand binding domain; hPXR, human pregnane X receptor; qHTS, quantitative high-throughput screening; rPXR, rat pregnane X receptor; PXRE, PXR response element; RXR, retinoid X receptor; NPC, National Institutes of Health Chemical Genomics Center Pharmaceutical Collection; DMSO, dimethyl sulfoxide; FRD, flying reagent dispenser; TR-FRET, time-resolved fluorescence resonance energy transfer; SR12813, 3,5-di-*tert*-butyl-4-hydroxystyrene-β,β-diphosphonic acid tetraethyl ester; CRC, concentration response curve; SAR, structure-activity relationship; LC, liquid chromatography; MS, mass spectrometry; TFA, trifluoroacetic acid; CDK, cyclin-dependent kinase; PPAR-γ, peroxisome proliferator-activated receptor.

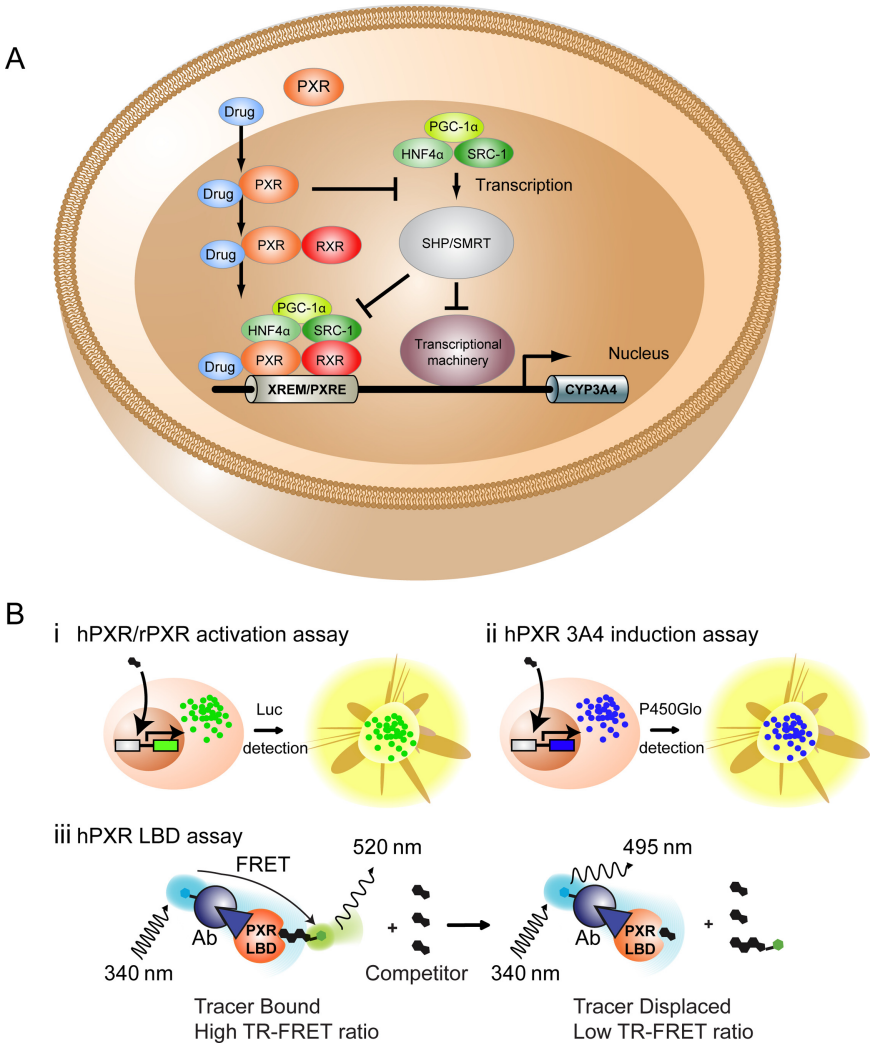

FIG. 1. Ligand-mediated PXR activation and CYP3A4 induction and assay schematic diagrams. A, upon ligand binding, PXR translocates into the nucleus. In the absence of PXR bound to ligand, an orphan nuclear receptor such as small heterodimer partner (SHP) and silencing mediator of retinoid and thyroid hormone receptors (SMRT) are transcribed by coactivators such as steroid receptor coactivator-1 (SRC-1), hepatocyte nuclear factor α (HNF4α), and peroxisome proliferator-activated receptor γ coactivator-1α (PGC-1α), resulting in the inhibition of CYP3A4 transcription. SHP/SMRT transcription is blocked by ligand-activated PXR, and the ligand-PXR complex forms a heterodimer with RXRα before stabilization by SRC-1 and other coactivators. The coactivator-PXR-RXRα complex binds the xenobiotic responsive enhancer molecule/PXRE (XREM/PXRE) region containing an everted repeat with a spacer of six nucleotides (ER6) in the proximal promoter and direct repeats with a three-nucleotide spacing (DR3) in the distal XREM upstream of the CYP3A4 transcription start site (Stanley et al., 2006; Sinz et al., 2007). Bi, the hPXR/rPXR activation assay relies on a luciferase reporter gene (green), which is downstream of the PXRE (gray). Upon ligand binding to the PXRE, the amount of luciferase enzyme (green dots) is quantified upon the addition of luciferin substrate and detection after cell lysis. Bii, the hPXR CYP3A4 induction assay relies on a luciferase-linked CYP3A4 promoter construct. Upon ligand binding to the PXRE, the amount of CYP3A4 enzyme expression (blue dots) is measured upon the addition of CYP3A4 substrate and detection after cell lysis. Biii, the hPXR LBD assay relies on the proximity of two fluorophores, including a Tb^{3+}-labeled antibody (Ab) which binds to the GST-tagged portion of the nuclear receptor (blue triangle). Excitation at 340 nm results in fluorescent emission at 495 nm and energy transfer to a fluorescein-labeled acceptor ligand capable of binding to the PXR LBD. The transfer of energy to the acceptor molecule results in fluorescent emission at 520 nm and a high TR-FRET ratio (520 nm/495 nm). In the presence of a PXR ligand (competitor), the displacement of the tracer molecule from the nuclear receptor is observed, resulting in a disruption of the energy transfer and loss of the TR-FRET signal.

induction of PXR and CYP3A4 (Jones et al., 2000). Pharmacological studies in primary hepatocytes also suggest that species-specific variation in CYP3A4 induction is not a consequence of CYP3A4 promoter structure, but rather of NRs such as PXR (Xie et al., 2000). Previous studies that have profiled compound-dependent PXR activation using species-specific hepatocytes found marked differences in ligand binding (Kocarek et al., 1993, 1995; Barwick et al., 1996; Jones et al., 2000). For example, rabbit and human PXR are activated by rifampicin; however, there are differences in PXR activation by other ligands such as dexamethasone (Jones et al., 2000). Thus, the validity of using animal models or nonhuman hepatocytes to predict CYP3A4 induction in humans has been questioned (Jones et al., 2000). Furthermore, the use of primary human hepatocytes is not feasible because of the unavailability and poor quality of human liver donors.

Despite knowledge regarding drug-drug interactions, little is known about the mechanism by which these agents activate PXR and induce CYP3A4 expression. Thus far, the majority of PXR and CYP3A4 activity profiling has come from computational prediction; however, there is a paucity of published experimental data on PXR activation and CYP3A4 induction by clinically used drugs, particularly those approved more than 10 years ago, when PXR was discovered. Furthermore, only a small fraction of the published data report EC_{50} values (Khandelwal et al., 2008). Thus, new in vitro methods to assess human PXR (hPXR) activation are warranted owing to the aforementioned reasons regarding species differences and availability and quality of human liver donors.

Because of the importance of PXR in xenobiotic metabolism and clinical pharmacology, a comprehensive publicly available database of its activity found in clinically used drugs would be tremendously valuable to both guide the use of currently prescribed pharmaceuticals and aid in the development of new drugs. Furthermore, rats are the preferred models for drug metabolism and pharmacokinetic studies; hence, rat-human PXR activation differences are important to identify and quantify. We have previously reported the profiling of a structurally diverse collection of up to 17,000 compounds for PXR binding and P450 activity (Shukla et al., 2009; Veith et al., 2009) using quantitative high-throughput screening (qHTS) (Shukla et al., 2009). In this study, we used qHTS to profile more than 2800 clinically used drugs and bioactive compounds for their ability to activate hPXR and rat PXR (rPXR) and induce human CYP3A4 using cell-based in vitro assays. The activities of these drugs at the cellular level (human) were further compared with their ability to bind the human PXR LBD at the protein level (Shukla et al., 2009) to identify compounds that directly bind to the LBD and those that potentially bind outside this region along the full-length PXR. Finally, we identified compounds that induced human CYP3A4 with an additional cell-based assay. The results obtained here will be clinically beneficial and can be used to prioritize compounds for further testing in in vitro and in vivo systems.

Materials and Methods

Cell Lines and Cell Culture Conditions. DPX-2 (used for hPXR activation and CYP3A4 induction studies) and rPXR cell lines were purchased from Puracyp (Carlsbad, CA). Construction of the DPX-2 cell line has been described previously (Raucy et al., 2002). In brief, HepG2 cells derived from human hepatocellular carcinoma cells were cotransfected with an expression vector containing the full-length coding region of hPXR, a PXR response element (PXRE), and a luciferase construct containing the CYP3A4 enhancer harboring distal and proximal promoters (Yueh et al., 2005). The PXRE is required for binding of the PXR and retinoid X receptor (RXR) heterodimer in the regulatory regions of target genes before activation. The luciferase construct containing the CYP3A4 enhancer (upstream of the luciferase reporter gene) is necessary for detection of CYP3A4 transcription, as measured by luminescence. The rPXR cell line was generated through cotransfection with an expression vector containing the full-length rPXR and a luciferase construct into a rodent hepatoma cell line (Sinz et al., 2007). Cell culture and assay medium were purchased from Puracyp, and the cells were maintained at 37°C under a humidified atmosphere and 5% CO_2.

National Institutes of Health Chemical Genomics Center Pharmaceutical Collection. The NPC collection (R. Huang, N. Southall, P. Shinn, A. Yasgar, Y. Wang, D. Nguyen, and C. Austin, manuscript in preparation) currently contains 2816 clinically used and bioactive small molecules, 52% of which are U.S. Food and Drug Administration-approved for human or animal use in the United States. The remaining drugs are either approved for use in other countries, such as Europe, Canada, or Japan, or are compounds that have been tested in clinical trials. The NPC library was prepared as 15 interplate titrations, which were serially diluted 1:2.236 in dimethyl sulfoxide (DMSO) (Thermo Fisher Scientific, Waltham, MA) in 384-well plates. The stock concentrations of the test compounds ranged from 10 mM to 0.13 μM. Transfer of the diluted compounds from 384-well plates to 1536-well plates was performed using an Evolution P^3 system (PerkinElmer Life and Analytical Sciences, Waltham, MA). Each treatment plate included concurrent DMSO and positive control wells and concentration-response titrations of controls, all occupying columns 1 to 4 (described in Supplemental Tables 1–3). During screening, the compound plates were sealed and kept at room temperature, whereas other copies were maintained at −80°C for storage.

hPXR and rPXR Activation. Summarized protocols for the hPXR and rPXR assays (Fig. 1Bi) can be found in Supplemental Tables 1 and 2, respectively. To measure PXR activation by a luciferase reporter readout, DPX-2 and rPXR cell lines were dispensed in white solid-bottom 1536-well plates (Greiner Bio-One North America, Monroe, NC) at 2000 cells/5 μl/well in assay medium using a flying reagent dispenser (FRD) (Aurora Discovery, Carlsbad, CA). Plates were incubated at 37°C for 5 h before transferring 23 nl of each compound from the NPC via a pin tool (Kalypsys, San Diego, CA), with final compound concentrations ranging from 7.5 nM to 46 μM. The final concentration of DMSO in the culture medium was <0.5%. Positive controls used to assess maximal response were rifampicin and dexamethasone for the hPXR and rPXR assays, respectively. All positive control compounds in the primary screens were also used as positive controls in the respective follow-up studies. The plates were incubated with compound for 24 h. Then 5 μl of One-Glo luciferase reagent (Promega, Madison, WI) was added to the plates, and the plates were incubated at room temperature for 30 min before reading on a ViewLux plate reader (PerkinElmer Life and Analytical Sciences).

CYP3A4 Induction Assay. A summarized protocol for Fig. 1Bii can be found in Supplemental Table 3. CYP3A4 induction, a luciferase reporter readout, was measured separately from PXR activation in DPX-2 cells using P450-Glo Screening Systems (Promega). In brief, DPX-2 cells were dispensed in white solid-bottom 1536-well plates at 2000 cells/5 μl/well in assay medium using an FRD. Next, the plates were incubated for 3.5 h before addition of 23 nl of each compound in the NPC. In addition, 1 μl of luciferin assay substrate was added to the cells and incubated at 37°C for 3 h. Then 5 μl of P450-Glo reagent was added to plates, and the plates were incubated at room temperature for 30 min before reading on the ViewLux plate reader. This particular reagent is robust and has been used previously for CYP3A4 profiling (Veith et al., 2009) with little to no fluorescence interference. Rifampicin was the positive control used to assess maximal response in the CYP3A4 induction assay. The positive control compound in the primary screens was also used as a positive control in the respective follow-up studies.

Determining Induction of CYP3A4 in Cryopreserved Human Hepatocytes. The procedure for thawing and culturing plateable cryopreserved human hepatocytes was performed as described in instructions for use from Celsis In Vitro Technologies (Chicago, IL) product information. In brief, cryopreserved human hepatocytes were thawed at 37°C for approximately 2 min and transferred into 5 ml of *InVitro*GRO CP medium at 37°C. The hepatocyte suspension was counted for viability and cell concentration using trypan blue exclusion. Cell density was diluted to a final concentration of 0.5×10^6 viable cells/ml. Cells were dispensed into 96-well BD BioCoat collagen I-coated culture plates (BD Biosciences, San Jose, CA) at a final density of 50,000 viable hepatocytes/well. On day 2 of culture, BD Matrigel (BD Biosciences) was added to the culture at 0.25 mg/ml protein in *InVitro*GRO CP medium. On days 3 and 4, cells were incubated with the positive control rifampicin (25 μM) in *InVitro*GRO HI medium to induce CYP3A4 protein levels or with test compound in a seven-point dosing range from 0.033 to 33 μM for rimexolone, oxatomide, colforsin, nilvadipine, and famprofazone and 0.01 to 100 μM for bumecainum. Vehicle control wells were incubated with 0.5% DMSO in *InVitro*GRO HI medium. On day 5, medium was removed, and metabolism was determined using P450-Glo CYP3A4 with Luciferin-IPA (Promega) according to the manufacturer's instructions for use. After a 30-min incubation with Luciferin-IPA substrate, medium was transferred to an opaque 96-well microtiter plate containing an equal volume of P450-Glo reaction buffer. The cell culture plate was washed with *InVitro*GRO Krebs-Henseleit buffer, and viability was determined using a CellTiter-Glo Luminescent Cell Viability Assay (Promega) according to the manufacturer's instructions for use.

PXR Ligand-Binding Domain Assay. The hPXR LBD assay (Fig. 1Biii) was performed with LanthaScreen time-resolved fluorescence resonance energy transfer (TR-FRET)-based technology (Invitrogen, Carlsbad, CA) and is described in detail elsewhere (Shukla et al., 2009). In brief, the assay was performed using the LanthaScreen TR-FRET PXR Competitive Binding Assay Kit, which contains the TR-FRET PXR assay buffer, Fluormone PXR Green (fluorescein-labeled PXR ligand), human PXR LBD (GST) (amino acids 111–434), and LanthaScreen Tb-anti-GST antibody. PXR LBD was diluted in the assay buffer to 1.5× the final recommended concentration to maintain optimal protein stability during the screening process in the 1536-well plate format. An FRD was used for all reagent dispensing. 3,5-Di-*tert*-butyl-4-hydroxystyrene-β,β-diphosphonic acid tetraethyl ester (SR12813), a potent PXR agonist, was used as a positive control to assess maximal response in the assay. The control columns were arranged as described previously (Shukla et al., 2009).

Cytotoxicity Assay in DPX-2 Cells. Cell viability was measured using a luciferase-coupled ATP quantization assay of metabolically active cells (ATPlite 1step Luminescence Assay System; PerkinElmer Life and Analytical Sciences). Cells were dispensed at 2000 cells/5 μl/well in 1536-well white solid-bottom assay plates using an FRD. The assay plates were incubated at 37°C for 5 h to allow for cell attachment, followed by addition of compounds via a pin tool. After compound addition, plates were incubated for 24 h at 37°C. At the end of the incubation period, 5 μl of ATPlite reagent was added, plates were incubated at room temperature for 20 to 30 min, and luminescence intensity was determined using a ViewLux plate reader. Positive control columns were arranged as the following: column 1, concentration-response titration of tetraoctyl ammonium bromide from 2.8 nM to 92 μM; column 2, 92 μM tetraoctyl ammonium bromide; column 3, DMSO only; and column 4, 23 μM tetraoctyl ammonium bromide. Compounds with curve classes 1.1, 1.2, 2.1, or 2.2 were considered cytotoxic, whereas compounds with class 4 curves were considered inactive, and all other curve classes were considered inconclusive (see *Data Analysis and Follow-up Studies*).

Data Analysis and Follow-up Studies. Data normalization and curve fitting were performed as described previously (Shukla et al., 2009). Raw plate reads for each titration point were normalized relative to the following controls, which represented 100% response: 23 μM rifampicin (hPXR activation and CYP3A4 induction assays), 46 μM dexamethasone (rPXR), or 92 μM tetra-*n*-octylammonium bromide (cytotoxicity in DPX-2 cells) and DMSO only wells (0%). The concentration-response curves (CRCs) for every compound were fit to the Hill equation, yielding half-maximal inhibition (IC_{50}) or activation (EC_{50}) and maximal response (efficacy) values. Fitting of experi-

mental data to the Hill equation was amended for bell-shaped concentration response curves, which showed an initial increase in activity at low compound concentrations followed by a sharp decline at higher compound concentrations: concentrations greater than the concentration of maximal response were masked for regression purposes to determine the AC_{50} of the maximal response. There were a total of 34 plates in the primary qHTS screen, which included 15 plates corresponding to each concentration per NPC library set and one DMSO-only plate at the beginning and end of each NPC library plate stack (final DMSO concentration of 0.45%).

Compounds from the primary qHTS screen were classified into four major curve classes according to quality of curve fit and efficacy as described previously (Shukla et al., 2009). Compounds with class 1.1, 1.2, 2.1, and 2.2 curves were associated with high-confidence and high-quality CRCs. The compounds in the aforementioned curve classes were considered as active, whereas compounds with class 4 curves were deemed inactive because they are not associated with any activity across the concentrations tested. All other curve classes (including those curves with single point activity) were deemed inconclusive. Hierarchical clustering of compound activity patterns was performed with Spotfire DecisionSite 8.2 (TIBCO Spotfire, Somerville, MA) using correlation of the log EC_{50} values as the similarity metric. Compounds that were associated with CRC classes 1 to 3 in at least three assays were included for clustering.

Follow-up studies were performed on a new aliquot of sample to confirm sample integrity and assay reproducibility. Compounds that were class 4 in one test and class 1.1, 1.2, 2.1, or 2.2 (efficacy >50%) in another test were not considered as confirmed. All other cases were considered confirmed. In the follow-up studies, 72 compounds were cherry-picked from the original solutions and chosen on the basis of activities and structural diversity across the four assays. The compounds also had efficacy >50% and potency <10 μM across at least one assay with class 1.1, 1.2, 2.1, and 2.2 curves (see *Data Analysis and Follow-up Studies*). Compounds were prepared in duplicate 24-point 2-fold dilution titrations in DMSO, with final concentrations ranging from 0.11 pM to 92 μM. These 72 compounds (Supplemental Table 4) were retested in the hPXR, rPXR, CYP3A4 induction, and PXR binding assays. For more extensive investigation and confirmation of previous results, 26 of 72 compounds were ordered from commercial vendors and were retested in the respective assays in duplicate 24-point 2-fold dilution titrations. These compounds were chosen on the basis of potency <10 μM in at least one of four assays with curve classes 1.1, 1.2, 2.1, and 2.2, novel mechanism of action with regard to hPXR activation or CYP3A4 induction assays and no apparent cytotoxicity.

Of the 26 compounds retested, 8 were purchased from Sigma-Aldrich (St. Louis, MO): ciglitazone, colforsin, diclazuril, felodipine, oxatomide, tacrolimus, troglitazone and zearalanol. Nine compounds were purchased from Prestwick Chemical (Washington, DC): famprofazone, fenbendazole, fluorometholone, hydralazine hydrochloride, methacycline hydrochloride, methylprednisolone 6-α, rimexolone, terconazole, and thonzonium bromide. Hetacillin potassium and thiamylal sodium were purchased from MicroSource (Gaylordsville, CT). Plicamycin and sirolimus were provided by the National Cancer Institute (Bethesda, MD). Other compounds purchased were bumecainum (Asinex, Winston-Salem, NC), nilvadipine (Bosche Scientific, New Brunswick, NY), riodipine (Enamine, Kiev, Ukraine); suramin (Enzo Life Sciences, Inc., Farmingdale, NY), and zafirlukast (Toronto Research Chemicals, Inc., Ontario, ON, Canada). All compounds were considered confirmed between solution cherry-picked and reordered samples unless high confidence curve classes became inactive or vice versa between the follow-up assays.

SAR Analysis. *Clustering of compounds by activity patterns.* Compounds were clustered hierarchically based on their log EC_{50} patterns from the primary screen across the four PXR assays within Spotfire DecisionSite 8.2 using the correlation of log EC_{50} values as the similarity metric (Fig. 5A). To facilitate SAR analysis, a simplified clustering of compound activity profiles was performed as follows: each compound was converted into a [0, 1] bit string with length 4 that represents its activity profile, with each bit corresponding to activity in a PXR assay. A bit was set to 1 if the compound was class 1 to 3 in the corresponding PXR assay and 0 if the compound was class 4. Eight different activity profiles (or bit patterns) were observed from the data, and the compounds were categorized according to their activity pattern (Fig. 5B).

Clustering of compounds by structure. The NPC compounds were clustered using the self-organizing map algorithm based on similarity in their Daylight structural fingerprints, yielding 351 clusters (data not shown).

Compounds that cocluster by structure and activity. Compounds that belong to the same activity cluster may fall into several structure clusters, and the same is true for compounds that belong to the same structure cluster. Combining the two sets of clustering results, the NPC compounds were further segregated into 695 structure-activity clusters, such that each of these clusters contains structurally similar compounds that also share similar activity patterns. More than 70% of these structure-activity clusters contain only one compound. We further examined the clusters that contain at least four compounds and found 16 such clusters (data not shown).

Chemical Analysis for Compound Purity. Initial purity and identity determination was performed on a Waters Acquity liquid chromatography (LC)-mass spectrometry (MS) system (Waters, Milford, MA). A 2.2-min gradient of 5 to 100% acetonitrile [containing 0.025% trifluoroacetic acid (TFA)] in water (containing 0.05% TFA) was used with a 3-min run time at a flow rate of 0.5 ml/min. A Luna column (2.0 × 100 mm, with 2.5-μm particle size; Phenomenex, Torrance, CA) was used at a temperature of 45°C. Purity was determined using a photodiode array detector and an evaporative light scattering detector. Mass was determined using a Waters Micromass ZQ mass spectrometer with electrospray. Data were analyzed using Waters OpenLynx software. Samples with inconclusive data, which required additional purity and identity determination, were processed on a 1200 LC-MS system (Agilent Technologies, Santa Clara, CA). This system used a 6.8-min gradient of 4 to 100% acetonitrile in water, with TFA proportions similar to those of the Acquity run in both solvents, over an 8.5-min run time. A Luna column (3.0 × 100 mm, with 3.0-μm particle size; Phenomenex) was used at a temperature of 50°C. Purity determination was performed using a diode array detector (Agilent Technologies). Mass determination was performed using a Quadrupole LC-MS system (Agilent Technologies). Samples that could not be identified because of poor ionization were further analyzed using a time-of-flight mass spectrometer (Agilent Technologies). Mobile-phase conditions were similar with the exception of 0.1% formic acid replacing TFA. Molecular formulas were confirmed using electrospray ionization with Masshunter software (version B.02; Agilent Technologies).

Results

Profiling Clinically Used Drugs against Human PXR. In this study, we profiled more than 2800 compounds in the NPC for hPXR activity in a cell-based hPXR activation assay and an hPXR LBD assay (Shukla et al., 2009) (Fig. 1) in qHTS format. The hPXR activation assay was performed with rifampicin, a well known hPXR agonist, as a positive control. The assay performed well across 34 1536-well plates with an average rifampicin EC_{50} of 3.5 μM and signal/background ratio of 5.7 (Supplemental Table 4). A total of 310 compounds from the primary screen were classified as activators of hPXR on the basis of high confidence curve classes (see *Materials and Methods*) and EC_{50} values ≤30 μM, yielding a hit rate of 11% (Table 1). There were eight active compounds with potency values less than 1 μM; however, the majority of the compounds had potency values greater than 10 μM (Table 1). To confirm compound activity, 72 compounds with no cytotoxicity or luciferase inhibition (data not shown) were cherry-picked from their original solutions and retested in the hPXR assay (Supplemental Table 5). Activity was confirmed in 66 of the 72

TABLE 1

Potencies for active compounds from primary qHTS across assays

Curve classes 1.1, 1.2, 2.1, and 2.2.

Potency	hPXR	hPXR LBD	CYP3A4 Induction	rPXR
μM				
<1	8	8	13	9
1–10	124	98	86	79
10–32	178	88	113	87

TABLE 2

Confirmation of follow-up assays

Assay	Primary qHTS vs. Cherry-Pick[a]	Cherry-Pick vs. Reacquired Samples[b]
	%	
hPXR	92	100
hPXR LBD	99	92
rPXR	100	85
CYP3A4	97	100

[a] Of 72 compounds retested.
[b] Of 26 compounds retested.

retested compounds, yielding a confirmation rate of 92% (Table 2). Based on potency and novelty of compound mechanism with respect to PXR activity from the primary screen, 26 of the 72 compounds were chosen for further follow-up in the hPXR assay and ordered from commercial vendors. All compound structures were confirmed by LC-MS, and the purity of all compounds was 100% with the exception of fenbendazole (92%). Ten of the 26 compounds had EC_{50} values <15 μM (Supplemental Table 6), 3 of which were dihydropyridine calcium channel antagonists, nilvadipine, felodipine, and riodipine. Seven of the 26 compounds activated hPXR only at higher concentrations (i.e., EC_{50} values greater than 23 μM). In contrast, 9 compounds showed no activity in hPXR up to the highest concentration tested (46 μM), which is also true for the cherry-pick solution activities.

We have previously screened the entire NPC for PXR ligand binding, a complementary dataset to identify drugs that activate hPXR via binding to the LBD (Shukla et al., 2009). We sought to compare the results of these two assays to obtain more information on the mechanism of PXR activation, especially because both studies were performed in a dose-response format. The hPXR LBD assay identifies PXR activation by direct LBD binding, whereas the hPXR cell-based assay can identify compounds that activate hPXR either through direct ligand binding or through modulation of hPXR activation by signaling pathways (Lin et al., 2008). The primary qHTS of the hPXR LBD assay performed well, with a signal/background ratio of 3.1 and average EC_{50} of 0.44 μM for the positive control SR12813 (Supplemental Table 4). Of the 2816 NPC compounds, 194 (7%) produced high-quality CRCs (Table 1). The activities of 71 compounds of 72 retested from the original solution were confirmed, yielding a 99% confirmation rate between the primary and follow-up assays (Table 2). Twenty-four of the 26 selected compounds were confirmed, with suramin and zafirlukast being most potent (Supplemental Table 6).

We wanted to assess the concordance rate among active compounds in the hPXR and PXR LBD assays to evaluate how many compounds from the hPXR assay may bind directly to the PXR LBD. To be more inclusive when calculating the concordance rate, we assessed all compounds (non-curve class 4) that showed activity. Among the 2814 compounds screened from the NPC, 603 compounds demonstrated concordant activity in both assays, whereas 846 compounds demonstrated activity in either assay, indicating a concordance rate of 71.3% (603 of 846). There were 7 high-efficacy compounds active in both assays upon retesting, including ciglitazone and zafirlukast (Supplemental Table 6).

Species Selectivity of Drugs against hPXR and rPXR. Although compound-mediated hPXR activation is most important clinically, rPXR activation is equally important in drug development before drug metabolism and pharmacokinetic studies are generally first performed in the rat before data extrapolation to humans. The rPXR cell-based primary screen performed well, with a signal/background ratio of 4.7 and an average EC_{50} of 2.6 μM across the screen for the dexamethasone positive control (Supplemental Table 4). Of the 2816 compounds profiled, 175 (6%) produced high-confidence CRCs, approximately half of which had potency values <10 μM (Table 1). Seventy-two compounds were cherry-picked and activities of all 72 were confirmed (Table 2).

Given the species-specific differences in hPXR and rPXR, we were interested in the concordance rate among active compounds in the two assays. There were 512 compounds that demonstrated concordant activity in both assays, whereas 750 compounds demonstrated activity in either assay, indicating a concordance rate of 68.3%. Among the 26 compounds retested in the follow-up study, plicamycin was the most potent compound that was only active in the rPXR assay (Supplemental Table 6; Fig. 2A), in which the bell-shaped CRC observed for plicamycin was not due to cytotoxicity. Other compounds active only in the rPXR assay included hydralazine hydrochloride and 6-α-methylprednisolone (Fig. 2A). In contrast, ciglitazone and troglitazone only showed activity in the hPXR specific assay (Supplemental Table 6; Fig. 2B). Rimexolone, fluorometholone, fenbendazole, and diclazuril were more potent in the rPXR assay (Fig. 3). These results indicate greater selectivity for rPXR in the follow-up assays, whereas compounds such as fluorometholone were uniquely active and potent in the primary assay (Table 3). In contrast, several compounds including thiamylal sodium, oxatomide, bumecainum, nilvadipine, riodipine, and felodipine displayed greater potency in the hPXR assay, indicating a greater selectivity for hPXR (Fig. 4; Supplemental Table 6).

Effect of Drugs on CYP3A4 Induction. Ligand binding to PXR frequently activates transcription of CYP3A4 and several other P450 genes (Ekins and Schuetz, 2002). To investigate the downstream mechanism of drug action, we screened the NPC with regard to human CYP3A4 induction. The primary qHTS measuring CYP3A4 induction performed well (Supplemental Table 4) and revealed 212 active compounds (8%) with high quality CRCs. Less than 50% of compounds displayed potency values <10 μM (Table 1). The activities of 70 compounds of 72 retested were confirmed, yielding a 97% confirmation rate (Table 2).

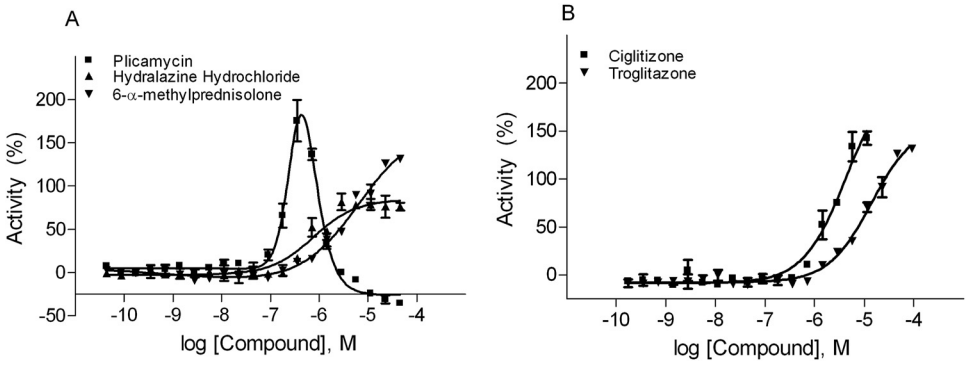

FIG. 2. Species-specific compounds involved in PXR activation. Compounds shown are taken from the set of 26 that were retested in each assay. Each CRC represents the average response of triplicates with error bars demonstrating the S.D. in the rPXR (A) and hPXR (B) assays.

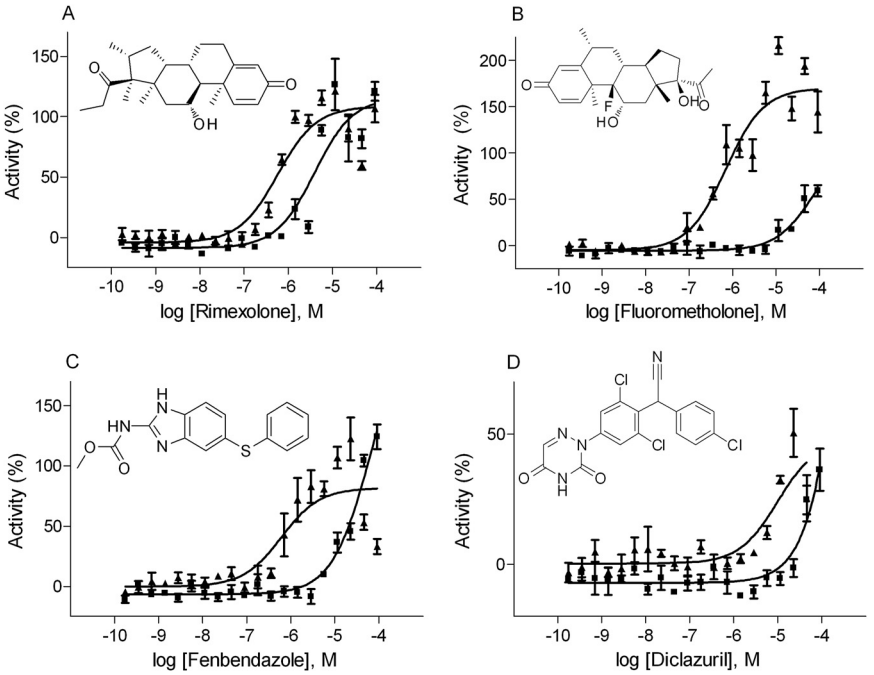

FIG. 3. Compounds selectively potent in the rPXR assay. Compounds shown are taken from the set of 26 that were retested in each assay. Each CRC represents the average response of triplicate determinations with error bars demonstrating the S.D. in the rPXR and hPXR assays for rimexolone (A), fluorometholone (B), fenbendazole (C), and diclazuril (D). ■, hPXR data; ▲, rPXR data.

There were 564 concordant compounds with regard to activity in the hPXR and CYP3A4 assays and 761 compounds that were active in either assay, resulting in a concordance rate of 74.1% (564 of 761). Of the 26 compounds retested in the CYP3A4 assay, three dihydropyridine calcium channel antagonists, riodipine, nilvadipine, and felodipine, showed the greatest potency (Supplemental Table 6). As expected, cluster analysis of EC_{50} patterns revealed the closest similarity between the hPXR activation and CYP3A4 induction assays with regard to compound activity profiles (Fig. 5A). Furthermore, linear regression, performed using the $\log_{10}$ transformed EC_{50} values derived from the 26 retested compounds, revealed a statistically significant correlation ($r^2 = 0.75$, $P < 0.0001$) between the hPXR activation and CYP3A4 induction assays. Taken together, these data suggest that a majority of compounds that activate hPXR also induce CYP3A4 for drug metabolism.

To test the effects of novel CYP3A4 DPX-2 inducers in cryopreserved primary hepatocytes, we tested six compounds, bumecainum, colforsin, famprofazone, nilvadipine, oxatomide, and rimexolone. All six compounds showed potent CYP3A4 induction in the cryopreserved primary human hepatocytes, confirming the DPX-2 results (Supplemental Table S6).

Identification of Structure-Activity Relationships Based on Activity Profiling. The NPC drugs were clustered both by similarity in structure and activity (EC_{50}) patterns (see *Materials and Methods* for details). Although most drugs showing similar activity patterns were structurally diverse, consistent with the promiscuous nature of PXR, several activity clusters contained drugs with common structural scaffolds (Fig. 5B). Figure 5B shows eight different activity profiles and structural classes associated with each activity profile.

The most prevalent profile was characterized by activity in the hPXR activation and CYP3A4 induction assays. There were 47 drugs having this profile (cluster 1, Fig. 5B), comprising four major structural classes: phenothiazines, dibenzazepines, thioxanthenes, and benztropines. Representative compounds from this profile are shown in Table 3. The second most prevalent number of drugs included those that displayed activity only in the hPXR LBD assay, comprising 30 drugs in three structural classes: unsaturated fatty acids, tetracyclines, and cephalosporins (cluster 2, Fig. 5B). Cluster 3 drugs demonstrated only CYP3A4 activity, typified by the hydroxyquinolines and cardiac glycosides. In contrast, 16 compounds in two major structural series, the steroid hormones and 4-anilinoquinazolines, comprised cluster 4, correlating with hPXR activation. Corticosteroids were associated with species-specific rPXR activity and included dexamethasone (Table 3), a well known rPXR activator (LeCluyse, 2001), among the 15 drugs included in cluster 5. Conversely, 9 drugs were active across all three human assays and included the imidazole antifungals (cluster 6). Seven compounds (dihydropyridine calcium channel blockers), including nilvadipine, nifedipine, and riodipine, were pan-active across all four assays (cluster 7) and have been shown previously to activate hPXR (Drocourt et al., 2001). Interestingly, a second scaffold, which was part of the dihydropyridine calcium channel blockers, was not associated with CYP3A4 activity (cluster 6). Variations in the substi-

TABLE 3

Representative species-specific compounds across activity groups

Cluster No. (Cluster Name)	Compound	hPXR Potency[a]	CYP3A4 Induction Potency[a]	rPXR Potency[a]
			μM	
1 (Phenothiazines)	Tropanyl 3,5-dimethylbenzoate	3.5	15.8	Inactive
1 (Thioxanthenes)	Thiothixene hydrochloride	12.6	7.1	Inactive
1 (Benztropines)	*t*-Butylhydroquinone	12.6	2.0	Inactive
5 (Corticosteroids)	Carminomycin	Inactive	Inactive	2.8
5 (Corticosteroids)	Dexamethasone acetate	Inactive	Inactive	4.5
5 (Corticosteroids)	Fluorometholone	Inactive	Inactive	0.4

[a] Taken from the primary qHTS screen.

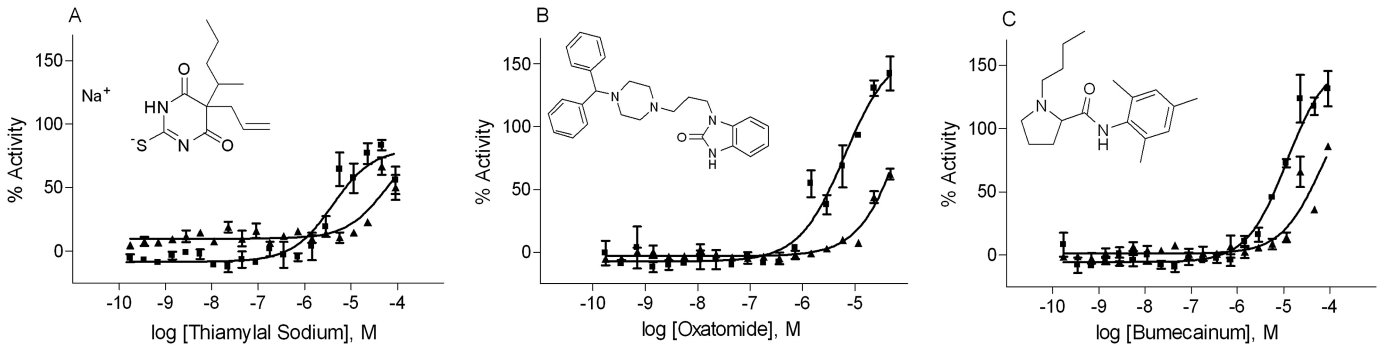

FIG. 4. Compounds that are selectively potent in the hPXR assay. Compounds shown are taken from the set of 26 that were retested in each assay. Each CRC represents the average response of triplicate determinations with error bars demonstrating the S.D. in the rPXR and hPXR assays for thiamylal sodium (A), oxatomide (B), and bemecainum (C). ■, hPXR data; ▲, rPXR data.

tution groups at the R_2 and R_4 positions seem to differentiate activity between clusters 6 and 7 and result in compound-specific behavior with regard to CYP3A4 induction. The corticosteroid/glucocorticoid scaffold was associated with cluster 8, for which activity is seen across all of the cell-based assays. Although this cluster shares a common backbone with the steroid and corticosteroid clusters associated with activity clusters 4 and 5, respectively, small changes in the ring structure and substituent groups have changed its activity profile across assays.

Discussion

In the present study, we have profiled a diverse array of clinically used drugs for species-specific PXR activation and CYP3A4 induction. Compounds identified and validated from the individual assays represent a range of known and novel PXR structurally divergent ligands. We observed that many drugs induced CYP3A4 through PXR activation and that the use of different assay formats and species-specific cell lines allowed for the construction of pharmacological profiles for PXR activity across each group.

To our knowledge, this is the first study to examine a large set of clinically approved drugs in a qHTS format to identify inducers of PXR and CYP3A4. The assays used were highly robust and allowed us to directly compare hPXR and rPXR activation at the cellular level. The use of stably transfected cell lines containing the PXR coding region and CYP3A4 promoter and enhancer elements to identify CYP3A4 inducers has been validated previously (Raucy et al., 2002; Yueh et al., 2005; Sinz et al., 2007). In a recent study, the use of in vitro cell-based methods that measure nuclear receptor activation has been demonstrated as a reliable method of identifying P450 inducers in a species-specific manner (Mueller et al., 2010).

It is worth noting that comparisons between different assay formats may produce discrepant results and warrant interrogation when data are interpreted. For example, compounds that were active in the hPXR assay and negative in the hPXR LBD assay may not have been able to displace the tracer molecule, thus appearing inactive. There are well known examples, such as docetaxel and paclitaxel, for which compound binding in one assay does not correlate to PXR binding in cell-based transactivation assays (Harmsen et al., 2007; Sinz et al., 2008); thus, many research groups have replaced PXR radioligand binding assays with cell-based assays (Sinz et al., 2006). In any case, active compounds from the hPXR LBD assay that do not reproduce in a cell-based assay could act as antagonists, may not enter the cell, or may be degraded in the cellular milieu. Finally, there has been recent evidence regarding the modulation of hPXR through ligand binding and/or cell signaling pathways such as protein kinase pathways (Lin et al., 2008). One recent study (Lin et al., 2008) identified two cyclin-dependent kinase (CDK) inhibitors that strongly activated hPXR in a cell-based transactivation assay but only weakly activated PXR in the same binding assay format used in our study. This finding indicates that direct hPXR binding is not completely responsible for hPXR activation due to CDK pathway inhibition, which otherwise negatively regulates hPXR activity (Lin et al., 2008). Although we do not have many CDK inhibitors represented in our NPC collection, compounds that are only active in the hPXR assay or have different potencies between the hPXR and hPXR LBD assays will warrant further functional investigation with regard to hPXR modulation via other pathways.

Active compounds in the hPXR cell-based assay that did not induce CYP3A4 could indicate a true effect or a CYP3A4 inhibitor that first binds PXR. Additional factors, such as negative feedback of CYP3A4 expression and other biochemical limitations with regard to the degree of CYP3A4 expression elicited by PXR activation (Luo et al., 2002), may have contributed to inactivity in the CYP3A4 induction assay. There were a few compounds that did not show PXR activation but demonstrated CYP3A4 induction (Supplemental Table 5); however, the majority of these demonstrated low efficacy and potency. Upon retesting from commercial vendors (Supplemental Table 6), there were no compounds that showed such an effect.

Our primary screening confirmed several compounds known to activate PXR, such as rifampicin, an antibiotic used in the treatment of tuberculosis. These results are consistent with a previous finding that rifampicin strongly activates PXR and induces CYP3A4 in HepG2 cells (Yasuda et al., 2008). Ritonavir, a protease inhibitor known to activate hPXR (Luo et al., 2002), was active in the hPXR assay with an EC_{50} value of 4 μM. Among the 26 compounds retested in our study, the majority are novel with regard to prior knowledge concerning species-specific and common activators of PXR. Rimexolone is a corticosteroid and anti-inflammatory agent used in eyedrops to reduce intraocular pressure (Kavuncu et al., 2008). This compound showed activity in both cell-based hPXR and rPXR assays and is a novel inducer of PXR activity. Although the relationship between hPXR, rPXR, and rimexolone is novel, human and rodent PXR are generally hormonally regulated (Goodwin et al., 2002).

This study confirms that nilvadipine, a calcium channel blocker used in the treatment of hypertension, activated hPXR and induced CYP3A4 (Niwa et al., 2004). Two other calcium channel blockers, felodipine and riodipine, showed similar activity (Supplemental Table 5). Felodipine is a known CYP3A4 substrate and is a commonly used in vivo probe for clinical studies involving CYP3A4 and CYP3A5 induction (Sinz et al., 2008). We also found that these compounds were 3- to 6-fold more potent in the hPXR assay than in the rPXR assay, which provides useful information for species selectivity.

The antitumor compound plicamycin was one of the most potent compounds in the rPXR follow-up assay (Fig. 2; Supplemental Table 6). Plicamycin, also referred to as mithramycin, is a naturally occurring

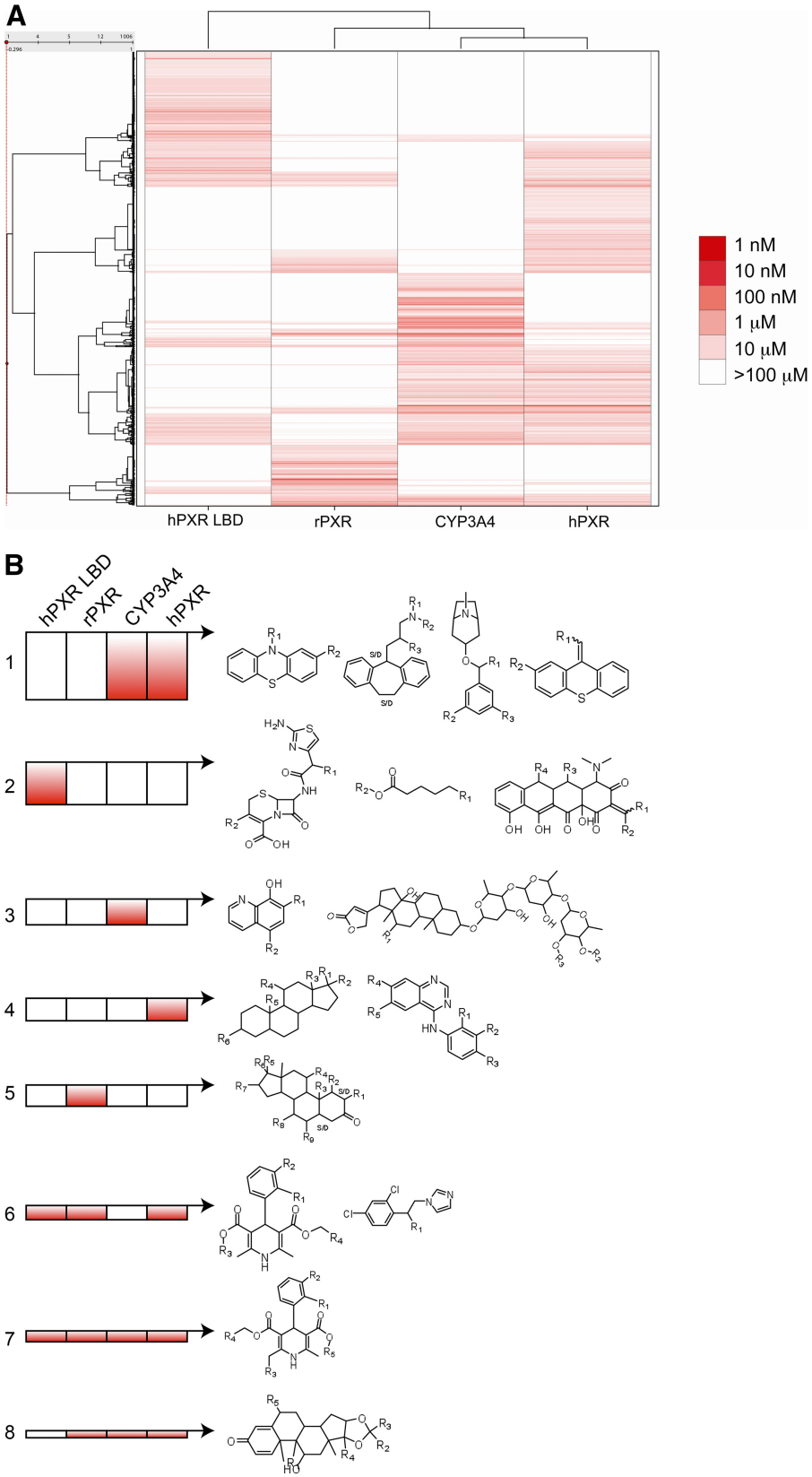

FIG. 5. Hierarchical clustering and SAR analysis of all cell-based and hPXR LBD assays. A, clustering was based on non-class 4 $\log_{10}$-transformed compound EC_{50} values across three or more assays. The cell-based assays generally cluster more closely together, followed by the hPXR LBD assay. B, each rectangle represents a cluster of structurally similar compounds. Eight activity clusters based on compound activity and potency across the four assays from the primary qHTS data are shown. Each cluster was associated with one to four structure classes. The white boxes indicate generally less potent/inactive compounds, and the red boxes indicate compounds that were generally more potent/active.

antibiotic used in the treatment of testicular carcinomas and acute myelogenous leukemia (Lahiri et al., 2008). This is a novel finding regarding species-specific induction of PXR by plicamycin, and further analogs can be studied with regard to drug development and coadministration with other drugs. The bell-shaped CRC of plicamycin could be explained by titration of coregulators interacting with rPXR in the HepG2 cell line, which would warrant further investigation. Ciglitazone, a PPAR-γ agonist used in the treatment of diabetes (Pershadsingh et al., 1993), demonstrated hPXR-specific induction (Fig. 2). This finding is consistent with a previous study showing severalfold (>5) ciglitazone-mediated

hPXR activation compared with mouse PXR activation (Vignati et al., 2004). Troglitazone, a PPAR-γ agonist and ciglitazone analog, is used in the treatment of type 2 diabetes (Jones et al., 2000) and showed hPXR-specific activation (Fig. 2). Previous studies have noted that these types of thiazolidinedione antidiabetic drugs assert their effects through activation of the PPAR-γ/RXR heterodimer (Lehmann et al., 1995). In addition, troglitazone activates hPXR at concentrations similar to those required to activate PPAR-γ, which provides additional evidence for interactions with other drugs such as oral contraceptives (Jones et al., 2000).

In addition to primary screening and follow-up assays, SAR analysis is a useful tool to potentially eliminate problematic chemotypes early in drug discovery (Sinz et al., 2008). SAR analysis revealed that most of the active compounds across the four assays are structurally diverse with multiple structural classes found within each activity group. Nevertheless, several classes of compounds that share the same chemical scaffolds were associated with different activity groups (Fig. 5B). Overall, our method was validated by the association of activity cluster 5 (activity in the rPXR assay only) with corticosteroids, which included the control compound dexamethasone. This approach was further validated by the association of hPXR activity (cluster 4) with steroid hormones. The structural classes associated with activity cluster 1 (benztropines, dibenzazepines, phenothiazines, and thioxanthenes) are commonly used as antipsychotic drugs and have limited data regarding their association with hPXR activation and CYP3A4 induction; thus, this may be a novel finding of the study. Terconazole, an azole-containing topical antifungal drug with anti-inflammatory properties (Liebel et al., 2006), demonstrated activity in the hPXR assay but not the CYP3A4 induction assay, suggesting regulation of CYP3A4 through other mechanisms.

As with the lack of a P450 isozyme diverse dataset before to a recent study (Veith et al., 2009), until now there has not been a publicly available comprehensive dataset of hPXR and rPXR activation and CYP3A4 induction by clinically used drugs to facilitate early drug discovery and avoid drug-drug interactions.

Acknowledgments

We thank Darryl Leja for illustrations, Bill Leister for quality control measurements of the compounds, and Dr. Judy Raucy for critical review of this article.

Authorship Contributions

Participated in research design: Shukla and Xia.

Conducted experiments: Shukla, Sakamuru, Moeller, Shinn, VanLeer, Xia.

Performed data analysis: Shukla, Huang, Xia.

Wrote or contributed to the writing of the manuscript: Shukla, Huang, Moeller, Auld, Austin, Xia.

References

Barwick JL, Quattrochi LC, Mills AS, Potenza C, Tukey RH, and Guzelian PS (1996) Trans-species gene transfer for analysis of glucocorticoid-inducible transcriptional activation of transiently expressed human CYP3A4 and rabbit CYP3A6 in primary cultures of adult rat and rabbit hepatocytes. *Mol Pharmacol* **50:**10–16.

Blumberg B and Evans RM (1998) Orphan nuclear receptors—new ligands and new possibilities. *Genes Dev* **12:**3149–3155.

Drocourt L, Pascussi JM, Assenat E, Fabre JM, Maurel P, and Vilarem MJ (2001) Calcium channel modulators of the dihydropyridine family are human pregnane X receptor activators and inducers of CYP3A, CYP2B, and CYP2C in human hepatocytes. *Drug Metab Dispos* **29:**1325–1331.

Ekins S, Reschly EJ, Hagey LR, and Krasowski MD (2008) Evolution of pharmacologic specificity in the pregnane X receptor. *BMC Evol Biol* **8:**103.

Ekins S and Schuetz E (2002) The PXR crystal structure: the end of the beginning. *Trends Pharmacol Sci* **23:**49–50.

Evans RM (2005) The nuclear receptor superfamily: a rosetta stone for physiology. *Mol Endocrinol* **19:**1429–1438.

Goodwin B, Redinbo MR, and Kliewer SA (2002) Regulation of cyp3a gene transcription by the pregnane X receptor. *Annu Rev Pharmacol Toxicol* **42:**1–23.

Harmsen S, Meijerman I, Beijnen JH, and Schellens JH (2007) The role of nuclear receptors in pharmacokinetic drug-drug interactions in oncology. *Cancer Treat Rev* **33:**369–380.

Jones SA, Moore LB, Shenk JL, Wisely GB, Hamilton GA, McKee DD, Tomkinson NC, LeCluyse EL, Lambert MH, Willson TM, et al. (2000) The pregnane X receptor: a promiscuous xenobiotic receptor that has diverged during evolution. *Mol Endocrinol* **14:**27–39.

Kavuncu S, Horoz H, Ardagil A, and Erbil HH (2008) Rimexolone 1% versus prednisolone acetate in preventing early postoperative inflammation after cataract surgery. *Int Ophthalmol* **28:**281–285.

Khandelwal A, Krasowski MD, Reschly EJ, Sinz MW, Swaan PW, and Ekins S (2008) Machine learning methods and docking for predicting human pregnane X receptor activation. *Chem Res Toxicol* **21:**1457–1467.

Kliewer SA (2003) The nuclear pregnane X receptor regulates xenobiotic detoxification. *J Nutr* **133:**2444S–2447S.

Kliewer SA, Moore JT, Wade L, Staudinger JL, Watson MA, Jones SA, McKee DD, Oliver BB, Willson TM, Zetterström RH, et al. (1998) An orphan nuclear receptor activated by pregnanes defines a novel steroid signaling pathway. *Cell* **92:**73–82.

Kocarek TA, Schuetz EG, and Guzelian PS (1993) Regulation of phenobarbital-inducible cytochrome P450 2B1/2 mRNA by lovastatin and oxysterols in primary cultures of adult rat hepatocytes. *Toxicol Appl Pharmacol* **120:**298–307.

Kocarek TA, Schuetz EG, Strom SC, Fisher RA, and Guzelian PS (1995) Comparative analysis of cytochrome P4503A induction in primary cultures of rat, rabbit, and human hepatocytes. *Drug Metab Dispos* **23:**415–421.

Lahiri S, Devi PG, Majumder P, Das S, and Dasgupta D (2008) Self-association of the anionic form of the DNA-binding anticancer drug mithramycin. *J Phys Chem B* **112:**3251–3258.

LeCluyse EL (2001) Pregnane X receptor: molecular basis for species differences in CYP3A induction by xenobiotics. *Chem Biol Interact* **134:**283–289.

Lehmann JM, McKee DD, Watson MA, Willson TM, Moore JT, and Kliewer SA (1998) The human orphan nuclear receptor PXR is activated by compounds that regulate CYP3A4 gene expression and cause drug interactions. *J Clin Invest* **102:**1016–1023.

Lehmann JM, Moore LB, Smith-Oliver TA, Wilkison WO, Willson TM, and Kliewer SA (1995) An antidiabetic thiazolidinedione is a high affinity ligand for peroxisome proliferator-activated receptor γ (PPARγ). *J Biol Chem* **270:**12953–12956.

Liebel F, Lyte P, Garay M, Babad J, and Southall MD (2006) Anti-inflammatory and anti-itch activity of sertaconazole nitrate. *Arch Dermatol Res* **298:**191–199.

Lin W, Wu J, Dong H, Bouck D, Zeng FY, and Chen T (2008) Cyclin-dependent kinase 2 negatively regulates human pregnane X receptor-mediated CYP3A4 gene expression in HepG2 liver carcinoma cells. *J Biol Chem* **283:**30650–30657.

Luo G, Cunningham M, Kim S, Burn T, Lin J, Sinz M, Hamilton G, Rizzo C, Jolley S, Gilbert D, et al. (2002) CYP3A4 induction by drugs: correlation between a pregnane X receptor reporter gene assay and CYP3A4 expression in human hepatocytes. *Drug Metab Dispos* **30:**795–804.

Moore LB, Parks DJ, Jones SA, Bledsoe RK, Consler TG, Stimmel JB, Goodwin B, Liddle C, Blanchard SG, Willson TM, et al. (2000) Orphan nuclear receptors constitutive androstane receptor and pregnane X receptor share xenobiotic and steroid ligands. *J Biol Chem* **275:**15122–15127.

Mueller SO, Fery Y, Tuschl G, and Schrenk D (2010) Species-specific activation of nuclear receptors correlates with the response of liver drug metabolizing enzymes to EMD 392949 in vitro. *Toxicol Lett* **193:**120–123.

Niwa T, Shiraga T, Hashimoto T, and Kagayama A (2004) Effect of nilvadipine, a dihydropyridine calcium antagonist, on cytochrome P450 activities in human hepatic microsomes. *Biol Pharm Bull* **27:**415–417.

Pershadsingh HA, Szollosi J, Benson S, Hyun WC, Feuerstein BG, and Kurtz TW (1993) Effects of ciglitazone on blood pressure and intracellular calcium metabolism. *Hypertension* **21:**1020–1023.

Raucy J, Warfe L, Yueh MF, and Allen SW (2002) A cell-based reporter gene assay for determining induction of CYP3A4 in a high-volume system. *J Pharmacol Exp Ther* **303:**412–423.

Shukla SJ, Nguyen DT, Macarthur R, Simeonov A, Frazee WJ, Hallis TM, Marks BD, Singh U, Eliason HC, Printen J, et al. (2009) Identification of pregnane X receptor ligands using time-resolved fluorescence resonance energy transfer and quantitative high-throughput screening. *Assay Drug Dev Technol* **7:**143–169.

Sinz M, Kim S, Zhu Z, Chen T, Anthony M, Dickinson K, and Rodrigues AD (2006) Evaluation of 170 xenobiotics as transactivators of human pregnane X receptor (hPXR) and correlation to known CYP3A4 drug interactions. *Curr Drug Metab* **7:**375–388.

Sinz M, Wallace G, and Sahi J (2008) Current industrial practices in assessing CYP450 enzyme induction: preclinical and clinical. *Aaps J* **10:**391–400.

Sinz MW, Pray D, and Raucy J (2007) The utility of stable cell lines to assess species differences in PXR transactivation. *Drug Metab Lett* **1:**147–152.

Stanley LA, Horsburgh BC, Ross J, Scheer N, and Wolf CR (2006) PXR and CAR: nuclear receptors which play a pivotal role in drug disposition and chemical toxicity. *Drug Metab Rev* **38:**515–597.

Timsit YE and Negishi M (2007) CAR and PXR: the xenobiotic-sensing receptors. *Steroids* **72:**231–246.

Veith H, Southall N, Huang R, James T, Fayne D, Artemenko N, Shen M, Inglese J, Austin CP, Lloyd DG, et al. (2009) Comprehensive characterization of cytochrome P450 isozyme selectivity across chemical libraries. *Nat Biotechnol* **27:**1050–1055.

Vignati LA, Bogni A, Grossi P, and Monshouwer M (2004) A human and mouse pregnane X receptor reporter gene assay in combination with cytotoxicity measurements as a tool to evaluate species-specific CYP3A induction. *Toxicology* **199:**23–33.

Watkins RE, Wisely GB, Moore LB, Collins JL, Lambert MH, Williams SP, Willson TM, Kliewer SA, and Redinbo MR (2001) The human nuclear xenobiotic receptor PXR: structural determinants of directed promiscuity. *Science* **292:**2329–2333.

Xie W, Barwick JL, Downes M, Blumberg B, Simon CM, Nelson MC, Neuschwander-Tetri BA, Brunt EM, Guzelian PS, and Evans RM (2000) Humanized xenobiotic response in mice expressing nuclear receptor SXR. *Nature* **406:**435–439.

Yasuda K, Ranade A, Venkataramanan R, Strom S, Chupka J, Ekins S, Schuetz E, and Bachmann K (2008) A comprehensive in vitro and in silico analysis of antibiotics that activate pregnane X receptor and induce CYP3A4 in liver and intestine. *Drug Metab Dispos* **36:**1689–1697.

Yueh MF, Kawahara M, and Raucy J (2005) High volume bioassays to assess CYP3A4-mediated drug interactions: induction and inhibition in a single cell line. *Drug Metab Dispos* **33:**38–48.

Zhang B, Xie W, and Krasowski MD (2008) PXR: a xenobiotic receptor of diverse function implicated in pharmacogenetics. *Pharmacogenomics* **9:**1695–1709.

Address correspondence to: Dr. Menghang Xia, National Institutes of Health, 9800 Medical Center Dr., Rockville, MD 20850. E-mail: mxia@mail.nih.gov